

Analytical solution of swell-induced surface instability for graded hydrogel layers

Zhigen Wu^{1,*}, Rui Huang², Yihua Liu¹, Hao Li¹

¹ School of Civil Engineering, Hefei University of Technology, Hefei, Anhui 230009, China

² Department of Aerospace Engineering and Engineering Mechanics, University of Texas, Austin, TX 78712, USA

* Corresponding author: zhigenwu@hfut.edu.cn

Abstract To obtain a theoretical solution for the critical condition of swell-induced surface instability, a graded hydrogel layer on a rigid substrate is divided into n fictitious sub-layers. By considering the boundary condition and interface continuity, a governing equation for surface instability is established. Hydrogel layers with the crosslink density varying in the thickness direction are examined in details. The results show that both the critical condition and the instability mode relate to the variation of the material properties. For a soft-on-hard graded layer, the onset of surface instability is determined by a short-wave mode with a limiting short wavelength. In contrast, for a hard-on-soft graded layer, a long-wave mode with a finite wavelength emerges as the critical mode at the onset of surface instability. The critical swelling ratio of the long-wave mode for hard-on-soft graded layers is considerably lower than that of the short-wave limit for soft-on-hard ones with the same shape factor. In addition, we found that both the critical swelling ratio and the characteristic wavelength depend on the gradient profile of material properties.

Keywords Hydrogel, Surface instability, Graded layer

1. Introduction

A hydrogel swells significantly when imbibing a large amount of solvent. Swell-induced surface instability of hydrogels has been observed by many researchers^[1-6], and a lot of theoretical and numerical studies have also been reported^[7-12]. Most of the theoretical studies to date have assumed the hydrogel to be homogeneous before swelling. Recently, a series of experiments by Guvendiren et al.^[7,13,14] have observed a rich variety of surface patterns (including creases and wrinkles) by using hydrogels with depth-wise crosslink gradients. It was found that both the critical condition and the characteristic length scale of the surface patterns depended on the crosslink gradient. Motivated by these experiments, we present a theoretical analysis on swell-induced surface instability of graded hydrogel layers, i.e., the layer with material properties varying in the thickness direction.

The critical condition for the onset of swell-induced surface instability in hydrogels has become an interesting subject of theoretical studies recently. By an energetic consideration, Hong et al.^[7] predicted a critical strain for surface creasing of an elastomer. More recently, Cao and Hutchinson^[12] found that surface wrinkling in an elastomer is highly unstable and extremely sensitive to imperfections that could significantly reduce the critical strain. For a hydrogel layer on a rigid substrate, the critical condition for swell-induced surface instability is similar to the elastomers under compression, but with subtle differences due to the interaction between solvent and the polymer network. Following a procedure similar to Biot's linear perturbation analysis, Kang and Huang^[9] predicted that the critical swelling ratio for wrinkling instability of a hydrogel layer varies over a wide range, depending on the material parameters.

The theoretical studies predict no characteristic length scale for the surface instability in homogeneous elastomers and hydrogels. By considering the effect of surface tension, Kang and Huang^[10] predicted a characteristic wrinkle wavelength that scales almost linearly with the

thickness of the hydrogel layer. Alternatively, a characteristic length scale may be introduced by assuming a thin skin layer at the surface of the hydrogel^[15] or more generally, by assuming a gradient of the material properties in the thickness direction. In this paper, by dividing a layer into fictitious sub-layers, we present theoretical results for the stability analysis for swelling of graded hydrogel layers. The results suggest that both the critical condition and the characteristic wavelength depend sensitively on the depth-wise variation of the material properties in the hydrogel layer.

2. Theory of confined homogeneous hydrogel layers

In this section we briefly review the homogeneously swelling and a linear perturbation analysis for confined hydrogel layers^[9,16,17].

2.1. Constrained swelling

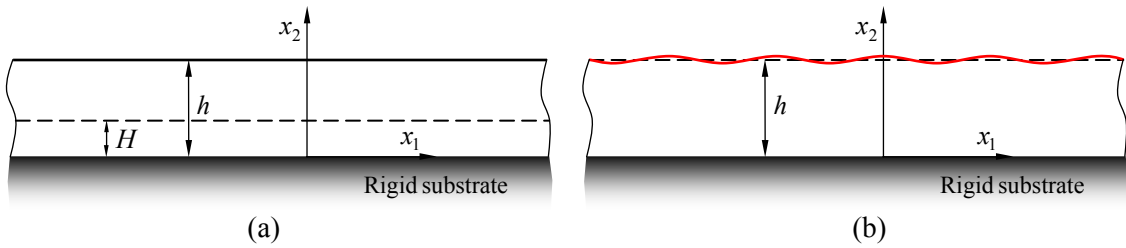


Fig. 1. Schematic of a hydrogel layer on a substrate: (a) a homogeneous swollen state; (b) a perturbation to the swollen state.

A homogeneous hydrogel layer is attached to a rigid substrate as shown in Fig. 1a. Since confined to the substrate, the hydrogel will swell only in the thickness direction with the thickness varying from H (at dry state) to h (at the swollen state). In the equilibrium state, the swelling ratio $\lambda_h = h/H$ can be obtained as a function of the chemical potential ($\hat{\mu}$) of external solvent in the following form^[9]:

$$\log\left(1 - \frac{1}{\lambda_h}\right) + \frac{1}{\lambda_h} + \frac{\chi}{\lambda_h^2} + N\Omega\left(\lambda_h - \frac{1}{\lambda_h}\right) = \frac{\hat{\mu} - p\Omega}{kT} \quad (1)$$

where $N\Omega$ and χ are two dimensionless parameters for material properties of the hydrogel, N represents the effective number of polymer chains per unit volume of the polymer network at the dry state, Ω is the volume per solvent molecule, χ reflects the interaction between the solvent molecules and the polymer, $\hat{\mu}$ is commonly a function of the temperature (T) and pressure (p), k the Boltzmann constant. Assuming an ideal gas phase ($p < p_0$) and an incompressible liquid phase ($p > p_0$), the external chemical potential is given by

$$\hat{\mu}(p, T) = \begin{cases} (p - p_0)\Omega, & \text{if } p > p_0, \\ kT \log(p/p_0), & \text{if } p < p_0, \end{cases} \quad (2)$$

where p_0 is the equilibrium vapor pressure of the solvent.

2.2. Linear perturbation fields

For a linear stability analysis, a two dimensional perturbation is assumed as small displacements added to the swollen state of the confined hydrogel layer (Fig. 1b), namely

$$u_1 = u_1(x_1, x_2) \quad \text{and} \quad u_2 = u_2(x_1, x_2). \quad (3)$$

The nominal stresses are obtained by the partial differentiation of the free energy with respect to the deformation gradient components as

$$s_{ij} \approx NkT[\tilde{F}_{ij} - (\lambda_h - \xi_h \varepsilon)H_{ij}] - pH_{ij} \quad (4)$$

where $\xi_h = \frac{1}{\lambda_h} + \frac{1}{N\Omega} \left(\frac{1}{\lambda_h - 1} - \frac{1}{\lambda_h} - \frac{2\chi}{\lambda_h^2} \right)$, $\varepsilon = \frac{\partial u_1}{\partial x_1} + \frac{\partial u_2}{\partial x_2}$, and $H_{ij} = \frac{1}{2} e_{ijk} e_{JKL} F_{jK} F_{kL}$.

Assume the perturbation displacements to be periodic in the x_1 direction, taking the form:

$$u_1 = U_1(x_2) \sin \omega x_1 \quad \text{and} \quad u_2 = U_2(x_2) \cos \omega x_1, \quad (5)$$

where ω is the wave number. Applying Eq. (5) to Eq. (4) and then inserting it to the mechanical equilibrium equation

$$\frac{\partial s_{ij}}{\partial X_j} = 0, \quad (6)$$

the equilibrium equation is finally derived as follows:

$$\lambda_h^2 U_1'' - \omega^2 (1 + \lambda_h \xi_h) U_1 - \omega \lambda_h \xi_h U_2' = 0, \quad (7)$$

$$\omega \lambda_h \xi_h U_1' + \lambda_h (\xi_h + \lambda_h) U_2'' - \omega^2 U_2 = 0. \quad (8)$$

And the perturbation displacement field can be solved from Eqs. (7) and (8) as

$$U_1(x_2) = A_1 e^{\alpha x_2 / \lambda_h} + A_2 e^{-\alpha x_2 / \lambda_h} + A_3 e^{\beta \alpha x_2} + A_4 e^{-\beta \alpha x_2}, \quad (9)$$

$$U_2(x_2) = -A_1 \lambda_h e^{\alpha x_2 / \lambda_h} + A_2 \lambda_h e^{-\alpha x_2 / \lambda_h} - A_3 \beta e^{\beta \alpha x_2} + A_4 \beta e^{-\beta \alpha x_2}, \quad (10)$$

where $\beta = \sqrt{(1 + \lambda_h \xi_h) / (\lambda_h^2 + \lambda_h \xi_h)}$.

3. A model of graded hydrogel layers

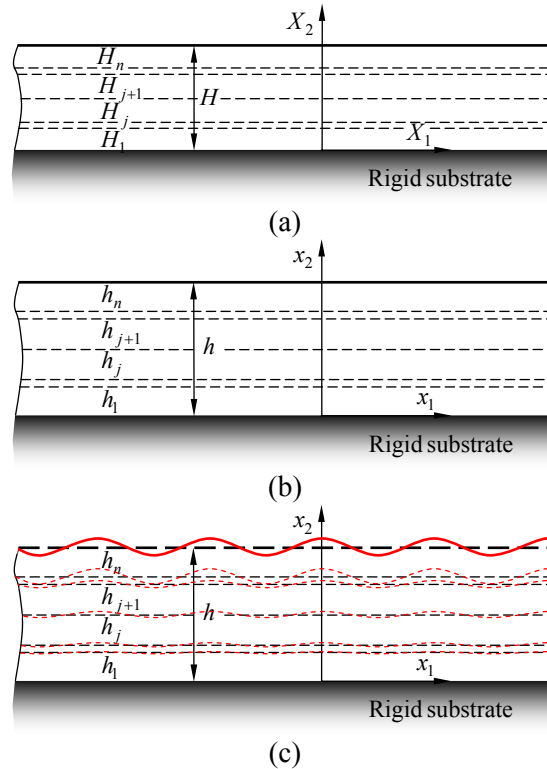


Fig. 2. Schematic of a graded hydrogel layer: (a) the dry state; (b) a transversely homogeneous swollen state; (c) a perturbation to the swollen state.

Consider a confined graded hydrogel layer as shown in Fig. 2. Set a Cartesian coordinate system in the dry state so that X_1 and X_3 are along the interface and X_2 in the thickness direction (Fig. 2a). Now we divide the layer into n fictitious sub-layers, each of which may have different thickness and different material properties. When n approaches infinity, the thicknesses of the sub-layers approach zero uniformly and also the laminated layers approach graded layer.

For the i th sub-layer considered as a homogeneous layer, the perturbation displacements (Fig. 2c) are in the form as Eqs. (9) and (10), i.e.,

$$U_1^{(i)} = A_1^{(i)} e^{\alpha x_2 / \lambda_{hi}} + A_2^{(i)} e^{-\alpha x_2 / \lambda_{hi}} + A_3^{(i)} e^{\beta_i \alpha x_2} + A_4^{(i)} e^{-\beta_i \alpha x_2}, \quad (11)$$

$$U_2^{(i)} = -A_1^{(i)} \lambda_{hi} e^{\alpha x_2 / \lambda_{hi}} + A_2^{(i)} \lambda_{hi} e^{-\alpha x_2 / \lambda_{hi}} - A_3^{(i)} \beta_i e^{\beta_i \alpha x_2} + A_4^{(i)} \beta_i e^{-\beta_i \alpha x_2}, \quad (12)$$

where $\beta_i = \sqrt{(1 + \lambda_{hi} \xi_{hi}) / (\lambda_{hi}^2 + \lambda_{hi} \xi_{hi})}$.

For the laminated layers, in addition to the boundary conditions, namely

$$U_1^{(1)} = U_2^{(1)} = 0, \quad \text{at } x_2 = 0, \quad (13)$$

$$(\xi_{hn} - \lambda_{hn}) \omega U_1^{(n)} + (\xi_{hn} + \lambda_{hn}) \frac{dU_2^{(n)}}{dx_2} = 0 \quad \text{and} \quad \frac{dU_1^{(n)}}{dx_2} - \omega U_2^{(n)} = 0, \quad \text{at } x_2 = h, \quad (14)$$

the perturbation displacements and the associated tractions must be continuous along the interface of any two adjacent sub-layers, namely

$$U_1^{(j)}(x_{hj}) = U_1^{(j+1)}(x_{hj}) \quad \text{and} \quad U_2^{(j)}(x_{hj}) = U_2^{(j+1)}(x_{hj}), \quad (15)$$

$$s_{12}^{(j)}(x_{hj}) = s_{12}^{(j+1)}(x_{hj}) \quad \text{and} \quad s_{22}^{(j)}(x_{hj}) = s_{22}^{(j+1)}(x_{hj}), \quad (16)$$

where $x_{hj} = h_1 + h_2 + \dots + h_j$ ($j = 1, 2, \dots, n-1$). Substituting Eqs. (11) and (12) into Eqs. (13)-(16) yields $4n$ linear homogeneous equations with respect to the coefficients $A_m^{(i)}$ ($m = 1 \sim 4, i = 1 \sim n$), which can be written in a matrix form:

$$\mathbf{D}\mathbf{A} = \mathbf{0}, \quad (17)$$

where \mathbf{D} is a $4n \times 4n$ matrix.

The critical condition for onset of the surface instability in the graded hydrogel layer is then obtained by setting the determinant of the matrix \mathbf{D} equal to zero, namely

$$\det(\mathbf{D}) = f(\omega H, \mu, N_i \Omega, \chi_i, k_i) = 0. \quad (18)$$

For each normalized wave number (ωH), we solve Eq. (18) to find the critical chemical potential μ_c , which depends on the material properties of sub-layer ($N_i \Omega, \chi_i$) as well as its volume fraction $k_i = H_i / H$. The swelling ratio of each sub-layer at the critical chemical potential, $\lambda_{hi}(\mu_c)$, is then calculated from Eq. (1). Subsequently, the general critical swelling ratio for the graded layer can be calculated from

$$\lambda_c = h / H = \sum_{i=1}^n k_i \lambda_{hi}. \quad (19)$$

4. Results and discussion

In this section, we apply the approach developed in the previous section to present the analytical results for the critical condition of surface instability for both hydrogel bilayers and graded hydrogel layers, and the effects of material properties are discussed as well.

4.1. Hydrogel bilayer instability

Fig. 3a plots the critical chemical potential as a function of the perturbation wave number for two bilayers (A and B), in comparison with a homogeneous layer. The corresponding critical swelling ratios are plotted in Fig. 3b. For the bilayers, the critical chemical potential varies with the perturbation wave number non-monotonically. If the top layer is softer than the underlayer ($N_2 < N_1$), the critical chemical potential has a local minimum μ_c^* , corresponding to a long-wave mode ($\omega = \omega^*$). The local minimum μ_c^* however is greater than the critical chemical potential at the short-wave limit ($\omega \rightarrow \infty$), i.e., $\mu_c^* > \mu_c^\infty$. Therefore, the onset of surface instability for such a bilayer (*soft-on-hard*) is expected to be determined by the short-wave limit. On the other hand, if the top layer is stiffer than the underlayer ($N_2 > N_1$), the minimum critical chemical potential occurs at a long-wave mode and is lower than the short-wave limit, i.e., $\mu_c^* < \mu_c^\infty$. Consequently, the critical condition for onset of surface instability for such a bilayer (*hard-on-soft*) is determined by a critical long-wave mode, with a characteristic length ($L^* = 2\pi/\omega^*$). In this case, the critical chemical potential for long-wave mode and the corresponding critical swelling ratio are considerably lower than that for a homogeneous layer.

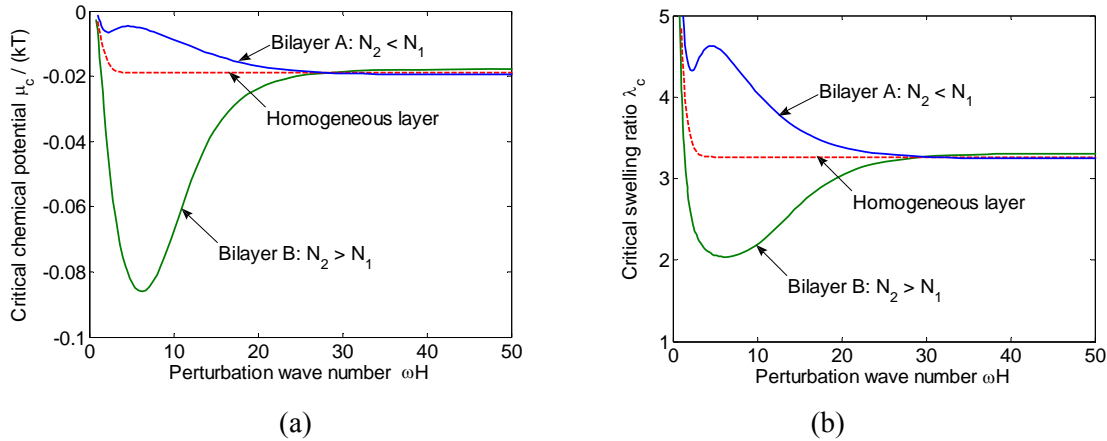


Fig. 3. (a) Critical chemical potential and (b) the corresponding swelling ratio versus the perturbation wave number for two hydrogel bilayers (A: $N_2\Omega = 4 \times 10^{-4}$; B: $N_2\Omega = 2 \times 10^{-3}$), both with $N_1\Omega = 10^{-3}$ and $k_1 = 0.9$, in comparison with a homogeneous hydrogel layer ($N\Omega = 10^{-3}$).

To highlight the distinct surface instability behaviors for the soft-on-hard and hard-on-soft hydrogel bilayers, a nonlinear finite element method developed previously^[8] is used to simulate swell-induced deformation and evolution of surface instability of the hydrogel bilayers, as shown in Fig. 4. The two models are identical in geometry, mesh, initial surface perturbation, boundary conditions, and volume fraction $k_1 = 0.9$. The common material properties are: $N_1\Omega = 10^{-3}$ and $\chi_1 = \chi_2 = 0.4$. The soft-on-hard bilayer, with $N_2\Omega = 4 \times 10^{-4}$, develops multiple surface creases without appreciable wrinkling (Fig. 4a and 4b), similar to that of a homogeneous layer^[9]. For the hard-on-soft bilayer, with $N_2\Omega = 10^{-2}$, the behavior is drastically different: the wrinkles grow significantly before creases form (Fig. 4c and 4d). The critical chemical potential or the critical swelling ratio for the onset of surface wrinkling in the hard-on-soft bilayer is considerably lower than that for surface creasing in the soft-on-hard bilayer.

Therefore, the two types of hydrogel bilayers (soft-on-hard vs hard-on-soft) exhibit distinct behavior at the onset of surface instability: for the soft-on-hard bilayer, with no characteristic length, surface wrinkling is highly unstable and is likely to collapse into creases; for the hard-on-soft

bilayer, surface wrinkling is stable with a finite wavelength.

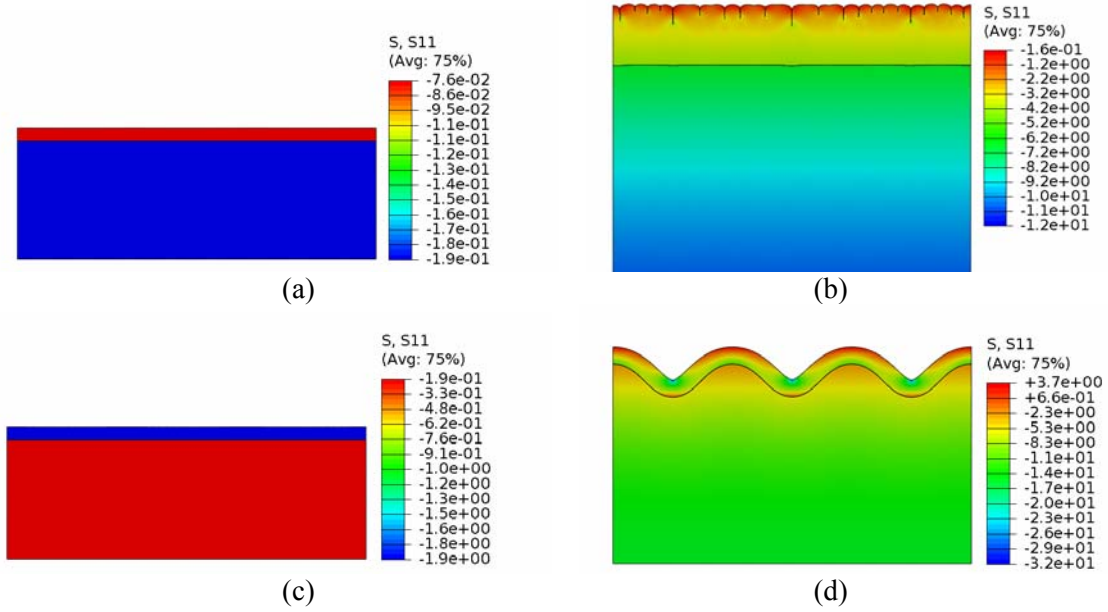


Fig. 4. Numerical simulations of swell-induced surface instability. (a) and (b): $\mu/kT = -1.158$ and -0.004 for a soft-on-hard bilayer ($N_1\Omega = 10^{-3}$ and $N_2\Omega = 4 \times 10^{-4}$); (c) and (d): $\mu/kT = -1.158$ and -0.1513 for a hard-on-soft bilayer ($N_1\Omega = 10^{-3}$ and $N_2\Omega = 10^{-2}$).

4.2. Graded hydrogel layer instability

To illustrate the effect of material parameters varying in the thickness direction on surface stability, we consider a graded hydrogel layer with linearly or exponential graded crosslink density. Since the effective number of polymer chains per unit volume is proportional to the crosslink density, we have

$$N(X_2) = N_{\text{bot}} + (N_{\text{sur}} - N_{\text{bot}}) \frac{X_2}{H}, \quad (20)$$

or

$$N(X_2) = N_{\text{bot}} + (N_{\text{sur}} - N_{\text{bot}}) \frac{\exp(\eta X_2 / H) - 1}{\exp(\eta) - 1}, \quad (21)$$

so that $N = N_{\text{bot}}$ at the bottom face of the hydrogel layer ($X_2 = 0$) and $N = N_{\text{sur}}$ at the surface ($X_2 = H$). The other material parameter, χ , is assumed to be a constant.

Fig. 5 shows the critical chemical potential and the critical swelling ratio as functions of the perturbation wave number for the graded hydrogel layer with $N_{\text{sur}}\Omega = 0.01$, $N_{\text{bot}}\Omega = 0.001$, $\chi = 0.4$, and the shape factor $\eta = 0$. The three curves in each figure represent the results for the graded layer divided into 5, 10, and 20 sub-layers, respectively. Similar to the hard-on-soft hydrogel bi-layer in Fig. 3, there exist the minimum critical chemical potential μ_c^* at a long-wave mode ω^* . It can also be observed that the results converge very fast, especially μ_c^* , ω^* , and the according critical swelling ratio λ_c^* coincide very well. Therefore, the enough accurate results may be obtained by using 20 sub-layers.

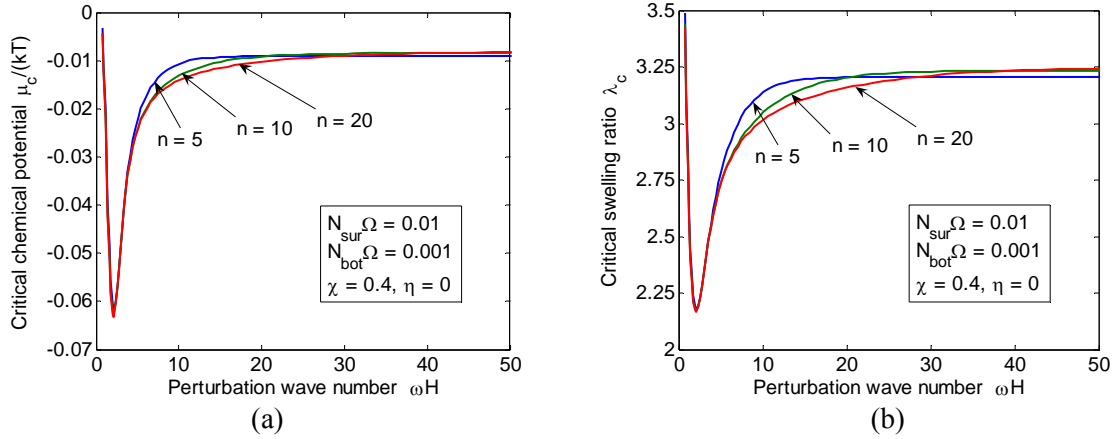


Fig. 5. (a) Critical chemical potential and (b) the corresponding swelling ratio versus the perturbation wave number for the graded hydrogel layer divided into 5, 10, 20 sub-layers, respectively.

The critical swelling ratios for different gradient profile with $\eta = -5, 0, 5$ are plotted in Fig. 6. It is interesting that critical swelling ratios relate to the shape factor η . For soft-on-hard graded layers ($N_{sur} < N_{bot}$), the critical swelling ratio decreases monotonically with increasing wave number, which is similar to the case of soft-on-hard bi-layers, but without a local minimum λ_c^* . The onset of surface instability is determined by short-wave limit and the according swelling ratio λ_c^∞ decreases as the shape factor increases (Fig. 6a). For hard-on-soft graded layers ($N_{sur} > N_{bot}$), the critical swelling ratio for the long-wave mode (λ_c^*) and the according wavelength (L^*) depend on gradient profile as shown in Fig. 6b, and apparently λ_c^* is considerably lower than λ_c^∞ for the soft-on-hard graded layer with the same shape factor. The critical swelling ratio for the long-wave mode (λ_c^*) varies with the shape factor η monotonically as shown in Fig. 7a. The swelling ratio decreases as the shape factor increases. However, the wavelength of the critical long-wave mode ($L^* = 2\pi / \omega^*$), normalized by the layer thickness H , first increases and then decreases with the increasing shape factor η as plotted in Fig. 7b.

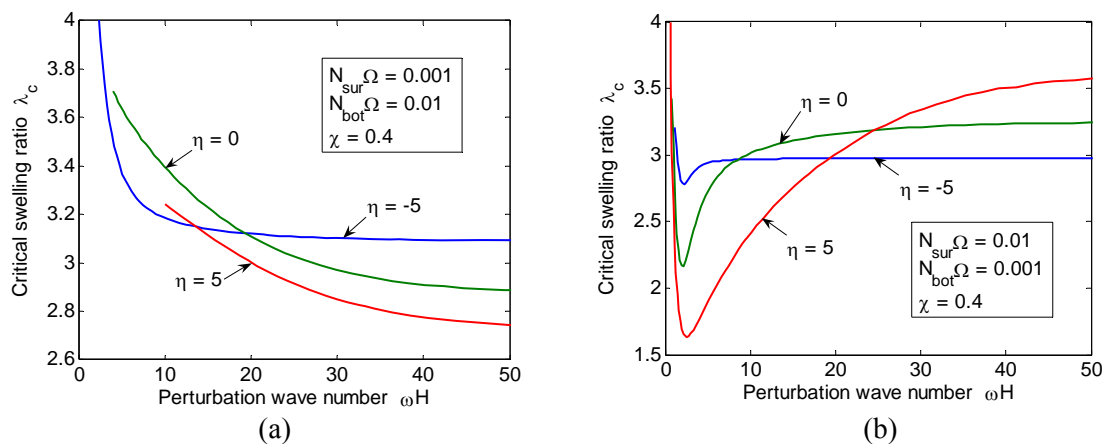


Fig. 6. Critical swelling ratio obtained by 20 sub-layers versus the perturbation wave number for: (a) soft-on-hard and (b) hard-on-soft graded hydrogel layers with different shape factors.

From the results for graded hydrogel layers, we can predict that the behavior at the onset of surface instability for graded hydrogel layers is similar to that of hydrogel bilayers, i.e., the soft-on-hard graded layer with no characteristic length and the hard-on-soft graded layer with a finite wavelength. Furthermore, both the critical swelling ratio and the wavelength depend on the gradient profile.

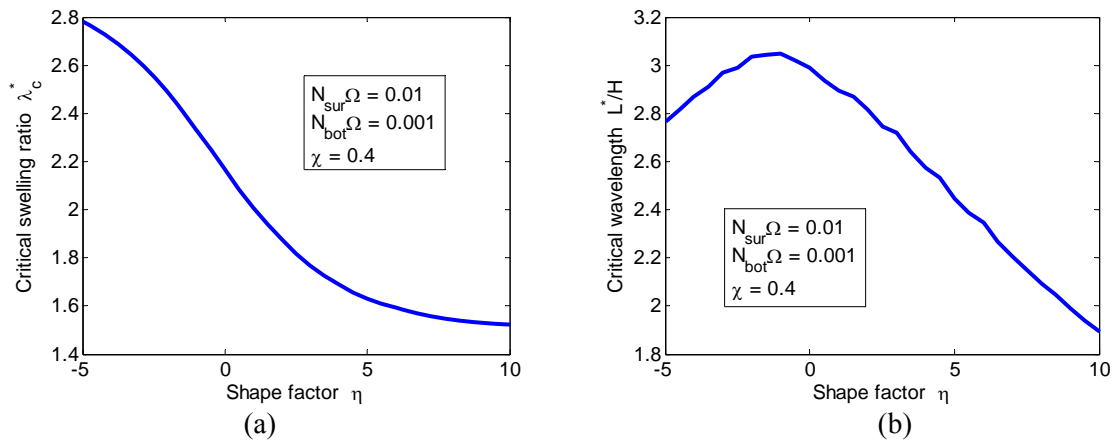


Fig. 7. (a) The critical swelling ratio for the long-wave mode and (b) the corresponding wavelength with shape factor η ranging from -5 to 10.

5. Conclusions

Based on the theory for homogeneous hydrogel layers, we presented a theoretical solution for the critical condition of swell-induced surface instability for a graded hydrogel layer on a rigid substrate. Graded hydrogel layers with the crosslink density varying in the thickness direction as well as hydrogel bilayers were examined as examples. The results show that both the critical condition and the instability mode depend on the variation of the material properties. For a soft-on-hard graded layer, the onset of surface instability is determined by a short-wave mode with a limiting short wavelength. In contrast, for a hard-on-soft graded layer, a long-wave mode with a finite wavelength emerges as the critical mode at the onset of surface instability. The critical swelling ratio of the long-wave mode for hard-on-soft graded layers is considerably lower than that of the short-wave limit for soft-on-hard ones with the same shape factor. In addition, we found that both the critical swelling ratio and the characteristic wavelength depend on the gradient profile of material properties.

Acknowledgements

The corresponding author gratefully acknowledges the financial support by Hefei University of Technology for his visiting as a scholar at The University of Texas at Austin.

References

- [1] E. Southern, A.G. Thomas, Effect of constraints on the equilibrium swelling of rubber vulcanizates. *J Polym Sci*, A3 (1965) 641–646.
- [2] T. Tanaka, S.-T. Sun, Y. Hirokawa, S. Katayama, J. Kucera, Y. Hirose, T. Amiya, Mechanical instability of gels at the phase transition. *Nature*, 325 (1987) 796–798.
- [3] V. Trujillo, J. Kim, R.C. Hayward, Creasing instability of surface-attached hydrogels. *Soft Matter*, 4 (2008) 564–569.
- [4] M. Guvendiren, S. Yang, J.A. Burdick, Swelling-induced surface patterns in hydrogels with gradient crosslinking density. *Adv Funct Mater*, 19 (2009) 3038–3045.
- [5] J. Dervaux, Y. Couder, M.-A. Guedeau-Boudeville, M. Ben Amar, Shape transition in artificial tumors: from smooth buckles to singular creases. *Phys Rev Lett*, 107 (2011) 018103.
- [6] S.S. Velankar, V. Lai, R.A. Vaia, Swelling-induced delamination causes folding of surface-tethered polymer gels. *ACS Appl Mater Interf*, 4 (2012) 24–29.

- [7] W. Hong, X. Zhao, Z. Suo, Formation of creases on the surfaces of elastomers and gels. *Appl Phys Lett*, 95 (2009) 111901.
- [8] M.K. Kang, R. Huang, A variational approach and finite element implementation for swelling of polymeric hydrogels under geometric constraints. *J Appl Mech*, 77 (2010) 061004.
- [9] M.K. Kang, R. Huang, Swell-induced surface instability of confined hydrogel layers on substrates. *J Mech Phys Solids*, 58 (2010) 1582–1598.
- [10] M.K. Kang, R. Huang, Effect of surface tension on swell-induced surface instability of substrate-confined hydrogel layers. *Soft Matter*, 6 (2010) 5736–5742.
- [11] J. Dervaux, M. Ben Amar, Buckling condensation in constrained growth. *J Mech Phys Solids*, 59 (2011) 538–560.
- [12] Y. Cao, J.W. Hutchinson, From wrinkles to creases in elastomers: the instability and imperfection-sensitivity of wrinkling. *Proc Royal Soc*, A468 (2012) 94–115.
- [13] M. Guvendiren, J.A. Burdick, S. Yang, Kinetic study of swelling-induced surface pattern formation and ordering in hydrogel films with depth-wise crosslinking gradients. *Soft Matter*, 6 (2010) 2044–2049.
- [14] M. Guvendiren, J.A. Burdick, S. Yang, Solvent induced transition from wrinkles to creases in thin film gels with depth-wise crosslinking gradients. *Soft Matter*, 6 (2010) 5795–5801.
- [15] E. Hohlfeld, L. Mahadevan, Unfolding the Sulcus. *Phys Rev Lett*, 106 (2011) 105702.
- [16] W. Hong, Z. Liu, Z. Suo, Inhomogeneous swelling of a gel in equilibrium with a solvent and mechanical load. *Int J Solids Struct*, 46 (2009) 3282–3289.
- [17] Z. Wu, N. Bouklas, R. Huang, Swell-induced surface instability of hydrogel layers with material properties varying in thickness direction. *Int J Solids Struct*, 50 (2013) 578–587.